

HMT-Grasp: A Hybrid Mamba-Transformer Approach for Robot Grasping in Cluttered Environments

Songsong Xiong¹, Hamidreza Kasaei¹

Abstract—Robot grasping, whether handling isolated objects, cluttered items, or stacked objects, plays a critical role in industrial and service applications. However, current visual grasp detection methods based on Convolutional Neural Networks (CNNs) and Vision Transformers (ViTs) struggle to adapt across various grasping scenarios due to the imbalance between local and global feature extraction. In this paper, we propose a novel hybrid Mamba-Transformer approach to address these challenges. Our method improves robotic visual grasping by effectively capturing both global and local information through the integration of Vision Mamba and parallel convolutional-transformer blocks. This hybrid architecture significantly improves adaptability, precision, and flexibility across various robotic tasks. To ensure a fair evaluation, we conducted extensive experiments on the Cornell, Jacquard, and OCID-Grasp datasets, ranging from simple to complex scenarios. Additionally, we performed both simulated and real-world robotic experiments. The results demonstrate that our method not only surpasses state-of-the-art techniques on standard grasping datasets but also delivers strong performance in both simulation and real-world robot applications.

I. INTRODUCTION

Robotic grasping has become increasingly important in industrial production and service applications [1], [2]. Tasks such as automated warehouse picking and household robots rely on accurate grasping to handle objects effectively. While early methods using hand-crafted features performed well in simple, controlled environments, modern robotic systems face more complex scenarios with diverse object shapes and unpredictable scenarios, making grasping a greater challenge [3].

Deep learning techniques, particularly Convolutional Neural Networks (CNNs) and Vision Transformers (ViTs), have greatly advanced computer vision tasks such as image classification, object detection, and segmentation [4], [5]. Researchers have leveraged these techniques to improve robotic grasp detection by utilizing their ability to extract crucial visual information. Early CNN-based grasp detectors [6]–[10] demonstrated notable improvements over hand-crafted methods, adapting to a wider variety of objects. However, CNNs focus mainly on local feature extraction, often missing the global context needed for grasping in more complex scenarios. To address this issue, Vision Transformers [11], [12] have been introduced in grasping tasks, offering enhanced global feature representation by capturing information across the entire input image. For instance, Wang et al. [13] and Dong et al. [14] employed transformers to encode target

scenes for robot grasping detection. While transformer-based approaches enhance global feature representation, they tend to decrease concern on local details as the model depth increases [15].

A more recent approach, Vision Mamba (ViM), balances global and local information more effectively than ViTs by incorporating Visual State Space (VSS) models [16]. While ViM improves spatial detail capture and focuses more on local features than transformers, its local feature extraction remains less refined than CNNs. In this work, we propose a hybrid Mamba-Transformer approach, integrating the strengths of Vision Mamba [17], transformers [18], and CNNs to enhance robotic grasp detection across various scenarios. By combining outputs from parallel CNNs and transformers as input to the Mamba encoder, our approach balances global and local feature representations, addressing the limitations of each model. Experimental results show that our method outperforms state-of-the-art techniques on multiple grasping datasets and delivers superior performance in both simulation and real-world robotic applications.

The main contributions of this paper can be summarized as follows:

- 1) We propose a novel hybrid Mamba-Transformer approach that integrates the strengths of Vision Mamba, transformers, and CNNs to improve robotic grasp detection. To the best of our knowledge, we are the first to explore the performance of the Mamba model in robotic grasping tasks.
- 2) We provide a comprehensive evaluation of our method on a diverse set of grasping datasets, demonstrating its effectiveness across various scenarios.

II. RELATED WORK

This section mainly reviews recent advancements in robotic grasp detection. Current research on robot grasp detection is primarily categorized into two approaches: CNN-based methods and ViT-based methods. Additionally, we provide a brief overview of recent progress with Vision Mamba in various domains.

A. Grasp Detection

CNN-Based Methods: Convolutional Neural Networks (CNNs) have been widely applied in robotic visual grasping tasks [9]. Early work by Lenz et al. introduced a two-step cascaded system that employed two deep neural networks to predict the grasp pose of objects. In this approach, numerous candidate grasps are first generated and then re-evaluated in a second step, which significantly slows down the detection

¹Department of Artificial Intelligence, University of Groningen, Groningen, The Netherlands
{s.xiong, hamidreza.kasaei}@rug.nl

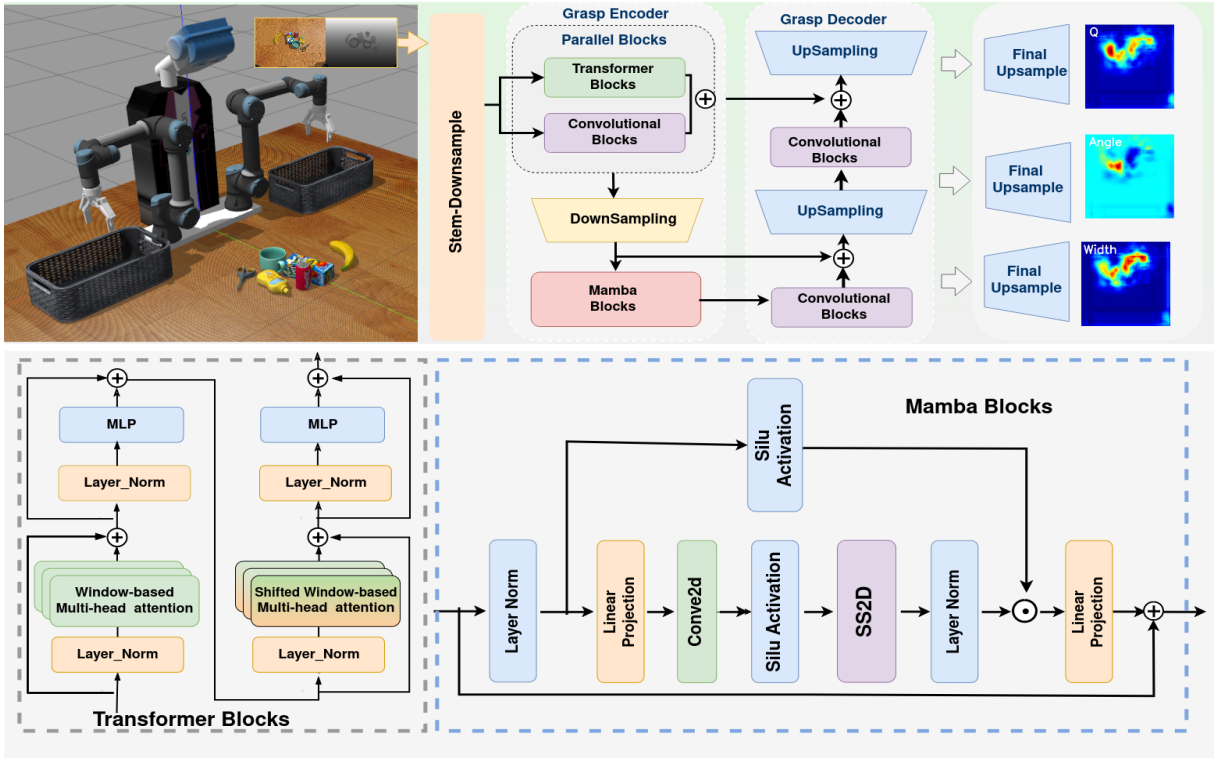


Fig. 1: Overview of the Hybrid Mamba-Transformer Architecture for Robotic Grasping in Cluttered Environments: The system consists of a Grasp Encoder and Grasp Decoder that employ parallel transformer and convolutional blocks, along with specialized Mamba blocks, to enhance both local and global feature extraction. The encoder down-samples the input to extract features, while the decoder uses up-sampling to predict the grasp quality (Q), angle, and width. The integration of Mamba blocks further improves feature extraction through Silu activation, SS2D layers, and linear projections, offering superior adaptability in complex grasping tasks.

process [13]. Subsequent research has leveraged CNNs to enhance object grasping performance by predicting grasp rectangles. Redmon et al. proposed a single-stage regression model that enabled real-time grasp detection [8]. To further improve accuracy, a ResNet-50-based grasp detector was introduced, demonstrating superior performance on the Cornell RGB-D dataset [19]. Datasets such as Jacquard [20] and Multi-Object [21] have contributed to enhancing the accuracy and generalization of CNN models in grasp detection. In addition, the Generative Grasping CNN (GG-CNN), designed to work with depth images, improved pixel-wise grasp quality in real-time scenarios. GR-ConvNet [10], proposed by Kumra et al., used n-channel inputs to detect antipodal grasps, achieving high accuracy on the Cornell and Jacquard datasets. Despite the effectiveness of CNN-based methods in grasp detection, a significant drawback is their tendency to lose global context due to the inherent structure of stacked convolutional layers [13].

ViT-Based Methods: Motivated by the success of Vision Transformers (ViTs) in object detection and image classification, researchers are increasingly exploring their potential for predicting object grasp poses in robotic tasks [13], [14], [22], [23]. Wang et al. [13] were among the first to propose the use of Swin-Transformers for visual grasp detection, employing them as both encoders and decoders with skip connections

to generate pixel-level grasp representations. Building on this, Dong et al. [14] also utilized Swin-Transformers for encoding, coupled with fully convolutional decoders to enhance grasp detection performance. In a more recent effort, Yenicesu et al. [23] introduced LITV2, a lightweight ViT model, to achieve real-time grasp detection. Compared to CNN-based methods, ViT-based approaches have demonstrated improved grasp detection accuracy. However, as the depth of transformer blocks increases, local-level information tends to gradually diminish [15].

B. Visual Mamba

Recently, Mamba, a novel State Space Model (SSM) initially developed for natural language processing (NLP) [24], has shown strong potential for efficiently modeling long sequences. This success has sparked increasing interest in applying SSMs to visual tasks. In particular, Mamba has been successfully implemented in various computer vision applications. For example, ViM [25], a Mamba-based architecture, operates on image patch sequences using a 1D causal scanning mechanism. However, the 1D scanning approach faces challenges in fully capturing global representations. To address this limitation, VMamba [26] introduces 2D-Selective-Scan, transforming images into sequences of patches for improved global feature extraction.

Inspired by these advancements, SegMamba [27] and VM-UNet [28] have successfully integrated visual state space models into encoders for medical image segmentation, contributing to notable performance improvements in this domain. Despite these developments, no prior work has explored the application of SSMs in robotic grasp detection. Given the strengths of mamba in capturing both global information and local details, alongside the complementary capabilities of transformers and CNNs, we designed a Mamba-Transformer approach to predict robotic grasp poses. Our method demonstrates superior grasp success rates compared to state-of-the-art transformer- and CNN-based approaches.

III. METHOD

In this section, we introduce a hybrid Mamba-Transformer architecture for robotic grasp detection. The overall structure of the model is shown in Fig. 1.

A. Grasp Representation

We define the grasp representation g , based on prior works [9], [13], as key parameters describing a successful grasp. Using a parallel-plate gripper constrained to the x - y plane, the grasp is represented by:

$$g = \{x_c, y_c, \theta, w, h\}$$

where (x_c, y_c) are the center coordinates of the grasp rectangle, w and h are the width and height, θ is the rotation angle. For an image I with n channels and dimensions $H \times W$, the predicted grasp is:

$$g_i = (x_i, y_i, \phi_i, w_i, q)$$

here, (x_i, y_i) are the coordinates, ϕ_i is the rotation angle, w_i is the grasp width, and q is the grasp quality. To convert image coordinates into the robot's reference frame, we apply a series of transformations:

$$g_r = t_{rc}(t_{ci}(g_i))$$

where t_{ci} transforms from image space to the camera frame using intrinsic parameters, and t_{rc} converts to the robot frame. The grasp information in the image is stored as a grasp map:

$$G = (Q, \Phi, W) \in R^{3 \times H \times W}$$

where Φ, W, Q represent the angle, width, and quality for each pixel. The hybrid Mamba-Transformer framework analyzes the n -channel image to determine the optimal grasping pose, focusing on predicting the grasp location, orientation, and width.

B. Grasp Encoder

The input tensor to the architecture has dimensions $[B, C, H, W]$, where B is the batch size, C is the number of channels, and H, W represent the height and width of the image. The tensor dimensions change as it passes through different layers of the model.

1) *Stem-Downsample Block*: Initially, the input tensor is processed by the *Stem-Downsample Block*, consisting of two *Conv2d* layers, each followed by BatchNorm (*BN*) and *SiLU* activations:

$$\begin{aligned} \hat{x} &= SiLU_1(BN_1(Conv2d_1(x))), \\ x &= SiLU_2(BN_2(Conv2d_2(\hat{x}))). \end{aligned} \quad (1)$$

2) *Parallel Convolutional-Transformer Blocks*: Following the StemDown Block, the output $(B, 96, \frac{W}{4}, \frac{H}{4})$ is processed through parallel *Transformer* and *Convolutional Blocks*.

Transformer Blocks: To capture global information, we employ the Swin Transformer block [11], which uses Window-based Multi-Head Self-Attention (*W-MSA*) and Shifted Window-based MSA (*SW-MSA*), followed by LayerNorm (*LN*) and Multi-Layer Perceptron (*MLP*).

$$\begin{aligned} \hat{x}_t^l &= W-MSA(LN(x_t^{l-1})) + x_t^{l-1}, \\ x_t^l &= MLP(LN(\hat{x}_t^l)) + \hat{x}_t^l, \\ \hat{x}_t^{l+1} &= SW-MSA(LN(x_t^l)) + x_t^l, \\ x_t^{l+1} &= MLP(LN(\hat{x}_t^{l+1})) + \hat{x}_t^{l+1}. \end{aligned} \quad (2)$$

Convolutional Blocks: To refine local features, a Double-Conv block is used, consisting of *Conv2D*, *BN*, and *ReSiLU* activations, where *ReSiLU* combines the outputs of ReLU and SiLU activations:

$$\begin{aligned} \hat{x}_c &= ReSiLU(BN(Conv2d(x))), \\ x_c &= ReSiLU(BN(Conv2d(\hat{x}))). \end{aligned} \quad (3)$$

3) *Downsampling*: To merge the information from the Transformer and Convolutional Blocks, we first compute the average of x_c and x_t , denoted as x_{fuse} . This is followed by a downsampling network consisting of *MaxPooling* and *DoubleConv* layers for further refinement:

$$\begin{aligned} \hat{x}_{fuse}^1 &= MaxPool(x_{fuse}), \\ \hat{x}_{fuse}^2 &= ReSiLU(BN(Conv2d(\hat{x}_{fuse}^1))), \\ \hat{x}_{fuse} &= ReSiLU(BN(Conv2d(\hat{x}_{fuse}^2))). \end{aligned} \quad (4)$$

The resulting fused tensor undergoes an additional Double-Conv operation, ensuring efficient downsampling and feature extraction.

4) *Mamba Blocks*: The fused and downsampled tensor \hat{x}_{fuse} with dimension $(B, 192, \frac{W}{8}, \frac{H}{8})$ is processed by the *Mamba Block*, inspired by the VM-UNet architecture [28]. The Mamba Block consists of LayerNorm (*LN*), Linear Projection (*LP*), *Conv2d*, *SiLU* activation, and 2D-Selective-Scan (*SS2D*). The computation is expressed as:

$$\begin{aligned} \hat{x}_m^{l,0} &= LN(x_m^{l-1}), \\ \hat{x}_m^{l,1} &= LN(SS2D(SiLU(Conv2d(LP(\hat{x}_m^{l,0}))))), \\ \hat{x}_m^l &= LP(SiLU(\hat{x}_m^{l,0}) \otimes \hat{x}_m^{l,1}) + x_m^{l-1}. \end{aligned} \quad (5)$$

In this formulation, the input x_m^{l-1} undergoes Layer Normalization before being processed by a series of operations, including a linear projection, convolution, and the SiLU activation. The resulting feature map is further refined using

the 2D-Selective-Scan (SS2D) mechanism, followed by an element-wise combination of the two branches. A final residual connection is applied to retain the input information and improve gradient flow during training. This structure aims to effectively capture spatial details and enhance the overall feature representation for subsequent stages of the network.

C. Grasp Decoder

After processing by the grasp encoder, the feature representation $(B, 192, \frac{W}{8}, \frac{H}{8})$ is passed to a *DoubleConv* block for further feature extraction. This *DoubleConv* block consists of *Conv2D*, *Batch Normalization (BN)*, and *ReSiLU* activation layers, similar to the ones used in the grasp encoder. During this step, the input and output dimensions remain unchanged. The output of the *DoubleConv* block is combined with the output x_m^{l-1} from the Mamba block. Mathematically, this can be expressed as:

$$x_{de}^{fuse,1} = DoubleConv(x_m^l) + x_m^{l-1} \quad (6)$$

The first fused output $(x_{de}^{fuse,1})$ is passed through an upsampling block. After upsampling, the output with dimensions $(B, 96, \frac{W}{4}, \frac{H}{4})$ is processed by another *DoubleConv* block for refinement:

$$x_{de}^{up,1} = DoubleConv(UpSample(x_{de}^{fuse,1})) \quad (7)$$

The first upsampled output $x_{de}^{up,1}$ is then summed with the output x_{fuse} from the parallel convolutional-transformer block in the grasp encoder, followed by an additional upsampling operation.

$$x_{de}^{up,2} = UpSample(x_{de}^{up,1} + x_{fuse}) \quad (8)$$

This process ensures the preservation and refinement of spatial details through feature refinement, skip connections, and upsampling. The resulting tensor $x_{de}^{up,2}$ with dimensions $(B, 48, \frac{W}{2}, \frac{H}{2})$ is further upsampled to generate pixel-level heatmap images for grasp prediction.

D. Grasp Prediction

In the final output of the HMT-Grasp detector, pixel-level heatmap images are generated for grasp representation. These include a grasp confidence map Q , a gripper angle map Θ , and a gripper width map W , all matching the input image size (224x224). Grasp posture estimation is formulated as a regression task, where the model learns the mapping $F : I \rightarrow \hat{G}$ to minimize the difference between predicted grasp heatmaps $\hat{G}(Q, W, \Theta)$ and ground truth G , with I as the input data. The loss function is defined as:

$$L = \sum_{i=1}^N \sum_{m \in \{Q, W, \Theta\}} \|\hat{G}_m^i - G_m^i\|^2 \quad (9)$$

where N represents the number of samples, and L_m^i denotes the ground truth for each sample.

The optimal grasp location is determined by selecting the position with the highest grasp confidence Q , as defined by:

$$Q_{pos}^* = \arg \max_{pos} Q \quad (10)$$

where Q_{pos}^* represents the chosen grasp location. The corresponding gripper angle Θ and width W are then extracted from the respective heatmaps.

IV. EXPERIMENTS

In this section, we present a comprehensive evaluation of our method through experiments on the Cornell, Jacquard, and OCID-Grasp datasets. We assess the impact of skip connections and Mamba blocks on performance and compare our approach to state-of-the-art methods. Additionally, we validate our method in both simulation and real-world robotic experiments. The grasp network has been implemented using PyTorch 2.0.1 with cuDNN 8.5.0.96 and CUDA 11.8. The model is trained end-to-end on an Nvidia RTX 4060 Ti GPU with 16GB of memory.

A. Dataset and Experiment setup

This section outlines the datasets used in the evaluation and provides relevant training details.

1) *Cornell Dataset and Training*: The Cornell dataset is one of the most widely used benchmarks for robotic grasping. It consists of 885 images of 250 real, graspable objects with a total of 8019 annotated grasps. The dataset contains RGB-D images and can be split using two different methods: image-wise and object-wise.

Given the relatively small size of the Cornell dataset, we employ 5-fold cross-validation to train and evaluate our model. To ensure robust performance, data augmentation is applied during training. The model is optimized using the Adam optimizer, with a learning rate initialized at 0.0002 and a batch size of 8. Training is carried out over 100 epochs to obtain the final model weights.

2) *Jacquard Dataset and Training*: The Jacquard grasp dataset is a large-scale dataset designed for robotic grasping tasks, comprising over 54,000 synthetic RGB-D images of more than 11,000 distinct objects. It includes approximately 1.1 million labeled grasps, generated using a physics-based simulation environment, providing diverse and comprehensive data for training grasping models.

We employ image-wise splitting to train and test our network, where 90% of the data is used for training, and the remaining 10% is reserved for testing. While we utilize the Adam optimizer, similar to the Cornell dataset training, we adjust the learning rate to 0.001 and set the batch size to 8. The network is trained over 200 epochs to obtain the final model weights.

3) *OCID Dataset and Training*: The OCID-Grasp dataset is a large-scale, real-world dataset created for robotic grasping in cluttered environments. It contains 1763 selected images with over 75,000 hand-annotated grasp candidates, classified into 31 object categories. The dataset is designed

to capture challenging grasping scenarios involving a variety of objects in cluttered settings.

We utilize 5-fold cross-validation, as in the Cornell dataset training, to train the networks and report average performance across the folds. The Adam optimizer is employed with a learning rate of 0.0004 and a batch size of 8. The network is trained for 70 epochs to achieve the final model weights.

B. Evaluation Metrics

Similar to previous studies [9], [10], [13], this work evaluates grasp detection using the following criteria:

- **Angle Difference:** The orientation difference between the predicted grasp and the ground-truth is less than 30°.
- **Jaccard Index:** The Jaccard index between the predicted grasp and the ground-truth is greater than 25%, calculated as:

$$J(g_{pre}, g_{truth}) = \frac{|g_{pre} \cap g_{truth}|}{|g_{pre} \cup g_{truth}|} \quad (12)$$

here, g_{pre} and g_{truth} denote the predicted and ground-truth grasp rectangles, respectively, with the intersection and union represented as $g_{pre} \cap g_{truth}$ and $g_{pre} \cup g_{truth}$.

C. Performance Comparison with State-of-the-Art Methods

To demonstrate the effectiveness of our approach, we compared it against state-of-the-art methods under consistent training and testing settings across the Cornell, Jacquard, and OCID-Grasp datasets.

1) *Grasping Performance on the Cornell Dataset:* We first evaluated our method on the Cornell dataset using 5-fold cross-validation. Table I presents the results for both image-wise (IW) and object-wise (OW) splits. Our proposed approach achieved a detection accuracy of 99.55%, outperforming other state-of-the-art methods in both splits. The superior

TABLE I: Results of our methods on the Cornell Grasping Dataset in image-wise and object-wise settings.

Method	Input	Accuracy (%)		Time (ms)
		IW	OW	
GG-CNN [9]	D	73.0	69.0	19
GPRN [29]	RGB	88.7	-	200
HybridGrasp [30]	RGB-D	93.2	89.1	-
GR-ConvNet [10]	RGB	96.6	95.5	19
GR-ConvNet [10]	RGB-D	97.7	96.6	20
TF-Grasp [13]	D	95.2	94.9	41.1
TF-Grasp [13]	RGB	96.78	95.0	41.3
TF-Grasp [13]	RGB-D	97.99	96.7	41.6
HRG-Net [31]	D	99.43	96.8	52.6
HRG-Net [31]	RGB	98.50	96.7	53.0
HRG-Net [31]	RGB-D	99.50	97.5	53.7
AE-GDN [32]	RGB	97.2	96.4	24.6
AE-GDN [32]	RGB-D	98.9	97.9	26.4
DCSFC-Grasp [33]	RGB-D	99.3	98.5	22
CGD-CNN [34]	RGB-D	97.8	96.6	19
QQGNN [1]	RGB-D	97.7	98.9	14.7
HMT-Grasp (Ours)	RGB	99.21	99.44	23.79
	D	99.32	99.55	22.25
	RGB-D	99.55	99.55	24.38

TABLE II: The Accuracy on Jacquard Grasping Dataset.

Years	Method	Input	Accuracy (%)
Morrison [9]	GGCNN2	RGBD	88.3
Kumra [10]	GR-ConvNet	RGB-D	91.0
Wang [13]	TF-Grasp	RGB-D	86.7
Ours	HMT-Grasp	D	93.0
	HMT-Grasp	RGB	90.4
	HMT-Grasp	RGB-D	93.3

performance of HMT-Grasp can be attributed to its ability to effectively capture both local and global features, enabling more precise grasp detection even in challenging scenarios. This result demonstrates the robustness and effectiveness of our approach across various input data configurations in the Cornell dataset.

2) *Grasping Performance on the Jacquard Dataset:* Data splitting for the Jacquard dataset varies across methods. For example, GGCNN2 uses 95% of the dataset for training, while TF-Grasp and GR-ConvNet use 90%, with minor differences in test splits. Additionally, distinctions between image-wise and object-wise splits are often unclear. To ensure fair comparisons, we reran all Jacquard experiments following the same protocol as state-of-the-art methods. The training and evaluation protocol is detailed in the *Jacquard Dataset and Training* section. As shown in Table II, our HMT-Grasp approach, using RGB-D input, achieved 93.3% accuracy, surpassing existing methods. The consistent improvement across different data splits reinforces the effectiveness of our hybrid architecture in capturing the critical features required for successful grasp prediction.

3) *Grasping Performance on the OCID-Grasp Dataset:* To validate our method in complex environments, we evaluated it on the OCID-Grasp dataset. The results, presented in Table III, follow the settings outlined in the *OCID Dataset and Training section*. Our approach, using RGB-D input, outperformed other methods, demonstrating its superior ability to handle complex grasping scenarios, and showing greater adaptability compared to ViTs and CNNs. The superior performance in this cluttered environment underscores the enhanced feature extraction capability of the Mamba blocks, which balance local and global information to enable more effective grasping decisions in difficult scenarios.

TABLE III: The Accuracy on OCID-Grasp Grasping Dataset.

Years	Method	Input	Accuracy (%)
Morrison [9]	GGCNN2	D	54.51
	GGCNN2	RGB	62.96
	GGCNN2	RGBD	64.66
Kumra [10]	GR-ConvNet	D	64.83
	GR-ConvNet	RGB	68.12
	GR-ConvNet	RGB-D	68.69
Wang [13]	TF-Grasp	D	41.63
	TF-Grasp	RGB	66.20
	TF-Grasp	RGB-D	66.02
Ours	HMT-Grasp	D	68.86
	HMT-Grasp	RGB	70.16
	HMT-Grasp	RGB-D	70.62

TABLE IV: Ablation experimental results from different skip-connections on the Cornell dataset.

Modality \ Connections	With Skip-connections	Without Skip-connections
Depth(%)	99.32	99.55
RGB(%)	99.21	99.20
RGB+Depth(%)	99.55	99.32

TABLE V: Ablation study for Mamba blocks on the Cornell dataset

Modality \ Model	With Mamba Blocks	Without Mamba Blocks
Depth(%)	99.32	97.51
RGB(%)	99.21	98.53
RGB+Depth(%)	99.55	98.87

D. Ablation Studies

To further investigate the impact of skip-connections and the Mamba block on grasp pose learning, we trained our network using 5-fold cross-validation on the Cornell dataset with image-wise splitting.

1) *Ablation study for skip-connections:* We firstly conducted experiments with and without skip-connections using our method across RGB, Depth, and RGB-D inputs. The detailed experimental results are presented in Table IV. The results show that incorporating skip-connections improves performance compared to omitting them, except for the Depth input.

2) *Ablation study for Mamba blocks:* Following the same procedure as the skip-connection ablation study, we evaluated the effect of the Mamba block on the Cornell dataset. The results, shown in Table V, demonstrate that the inclusion of Mamba blocks leads to superior performance across Depth, RGB, and RGB-D inputs compared to the model without Mamba blocks.

E. Simulation and Real Robot Experiments

In this section, we first conducted robot grasping experiments in the Gazebo using models. First, we performed 10 isolated experiments for each object by randomly spawning it within the robot’s workspace. The results, presented in Table VI, demonstrate the effectiveness of our method in

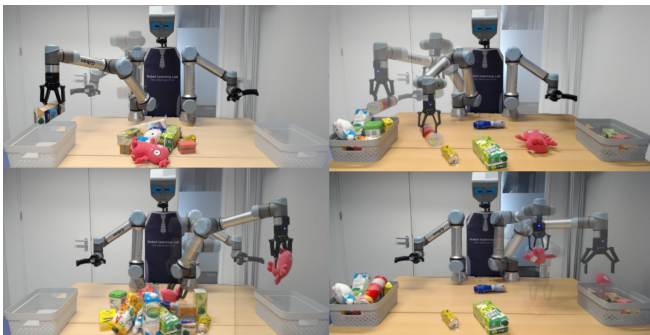


Fig. 2: An experiment of cleaning a table in robot applications in cluttered environments.



Fig. 3: Experiment setups: (left) simulation and (right) real robot.

grasping various objects. The reasons for failures can be attributed to the complexity of object shapes and material properties, such as sponges being soft and deformable, making it difficult for the grasp detection model to predict an optimal grasp configuration. As illustrated in Fig. 3, we also conducted 10 rounds of object grasping in cluttered scenarios for both simulation and real robots. In the case of simulation experiments, the robot was able to outperform the selected state-of-the-art with a 7% margin (65% vs 72%). The model’s ability to balance local and global feature extraction, thanks to the Mamba blocks, contributed significantly to its improved performance in complex scenarios. The real robot achieved a success rate comparable to the simulation results, with 67% successful grasps. The failures in real-world experiments were primarily due to object occlusion. In particular, many objects are partially occluded by others, leading to attempts to grasp objects at an inappropriate angle or position.

TABLE VI: Simulation Results: 20 simulations were performed for each object to assess the grasp success rate (%)

Objects	Pear	lemon	sponge	can_coke	Peach
GR-ConvNet [10]	80	75	85	80	75
HMT-Grasp	100	95	75	95	80
Objects	mug	scissor	tea	banana	flash
GR-ConvNet [10]	80	70	70	85	75
HMT-Grasp	70	95	80	85	90

V. CONCLUSION

This paper presents a hybrid Mamba-Transformer model for robotic grasping in complex scenarios. By combining Mamba, Transformers, and CNNs, our method overcomes the limitations of ViTs and CNNs in visual grasp detection. We conducted extensive evaluations on the Cornell, Jacquard, and OCID-Grasp datasets, where our model consistently outperformed state-of-the-art methods, achieving an accuracy of 99.5% on the Cornell dataset. These results demonstrate the superior adaptability and precision of our approach. Additionally, real-world robotic experiments further validated the method’s effectiveness in dynamic and complex environments, highlighting its potential for practical applications. Future work could focus on incorporating real-time feedback mechanisms to dynamically adjust grasp plans during execution.

REFERENCES

- [1] K. Fu and X. Dang, "Light-weight convolutional neural networks for generative robotic grasping," *IEEE Transactions on Industrial Informatics*, 2024.
- [2] D. Liu, X. Tao, L. Yuan, Y. Du, and M. Cong, "Robotic objects detection and grasping in clutter based on cascaded deep convolutional neural network," *IEEE Transactions on Instrumentation and Measurement*, vol. 71, pp. 1–10, 2021.
- [3] J. Zhao, L. Ye, Y. Wang, and H. Min, "Robot grasping using dilated residual convolutional neural network," in *2022 WRC Symposium on Advanced Robotics and Automation (WRC SARA)*. IEEE, 2022, pp. 133–139.
- [4] A. Khan, A. Sohail, U. Zahoor, and A. S. Qureshi, "A survey of the recent architectures of deep convolutional neural networks," *Artificial intelligence review*, vol. 53, pp. 5455–5516, 2020.
- [5] S. Khan, M. Naseer, M. Hayat, S. W. Zamir, F. S. Khan, and M. Shah, "Transformers in vision: A survey," *ACM computing surveys (CSUR)*, vol. 54, no. 10s, pp. 1–41, 2022.
- [6] Y. Jiang, S. Moseson, and A. Saxena, "Efficient grasping from rgb-d images: Learning using a new rectangle representation," in *2011 IEEE International conference on robotics and automation*. IEEE, 2011, pp. 3304–3311.
- [7] I. Lenz, H. Lee, and A. Saxena, "Deep learning for detecting robotic grasps," *The International Journal of Robotics Research*, vol. 34, no. 4-5, pp. 705–724, 2015.
- [8] J. Redmon and A. Angelova, "Real-time grasp detection using convolutional neural networks," in *2015 IEEE international conference on robotics and automation (ICRA)*. IEEE, 2015, pp. 1316–1322.
- [9] D. Morrison, P. Corke, and J. Leitner, "Learning robust, real-time, reactive robotic grasping," *The International journal of robotics research*, vol. 39, no. 2-3, pp. 183–201, 2020.
- [10] S. Kumra, S. Joshi, and F. Sahin, "Antipodal robotic grasping using generative residual convolutional neural network," in *2020 IEEE/RSJ International Conference on Intelligent Robots and Systems (IROS)*. IEEE, 2020, pp. 9626–9633.
- [11] Z. Liu, Y. Lin, Y. Cao, H. Hu, Y. Wei, Z. Zhang, S. Lin, and B. Guo, "Swin transformer: Hierarchical vision transformer using shifted windows," in *Proceedings of the IEEE/CVF international conference on computer vision*, 2021, pp. 10 012–10 022.
- [12] Z. Pan, J. Cai, and B. Zhuang, "Fast vision transformers with hilo attention," *Advances in Neural Information Processing Systems*, vol. 35, pp. 14 541–14 554, 2022.
- [13] S. Wang, Z. Zhou, and Z. Kan, "When transformer meets robotic grasping: Exploits context for efficient grasp detection," *IEEE robotics and automation letters*, vol. 7, no. 3, pp. 8170–8177, 2022.
- [14] M. Dong, Y. Bai, S. Wei, and X. Yu, "Robotic grasp detection based on transformer," in *International Conference on Intelligent Robotics and Applications*. Springer, 2022, pp. 437–448.
- [15] M. Raghu, T. Unterthiner, S. Kornblith, C. Zhang, and A. Dosovitskiy, "Do vision transformers see like convolutional neural networks?" *Advances in Neural Information Processing Systems*, vol. 34, pp. 12 116–12 128, 2021.
- [16] R. Xu, S. Yang, Y. Wang, B. Du, and H. Chen, "A survey on vision mamba: Models, applications and challenges," *arXiv preprint arXiv:2404.18861*, 2024.
- [17] J. Ruan and S. Xiang, "Vm-unet: Vision mamba unet for medical image segmentation. arxiv 2024," *arXiv preprint arXiv:2402.02491*.
- [18] Z. Liu, Y. Lin, Y. Cao, H. Hu, Y. Wei, Z. Zhang, S. Lin, and B. Guo, "Swin transformer: Hierarchical vision transformer using shifted windows," in *Proceedings of the IEEE/CVF International Conference on Computer Vision (ICCV)*, October 2021, pp. 10 012–10 022.
- [19] S. Kumra and C. Kanan, "Robotic grasp detection using deep convolutional neural networks," in *2017 IEEE/RSJ International Conference on Intelligent Robots and Systems (IROS)*. IEEE, 2017, pp. 769–776.
- [20] A. Depierre, E. Dellandréa, and L. Chen, "Jacquard: A large scale dataset for robotic grasp detection," in *2018 IEEE/RSJ International Conference on Intelligent Robots and Systems (IROS)*. IEEE, 2018, pp. 3511–3516.
- [21] F.-J. Chu, R. Xu, and P. A. Vela, "Real-world multiobject, multigrasp detection," *IEEE Robotics and Automation Letters*, vol. 3, no. 4, pp. 3355–3362, 2018.
- [22] Y. Han, R. Batra, N. Boyd, T. Zhao, Y. She, S. Hutchinson, and Y. Zhao, "Learning generalizable vision-tactile robotic grasping strategy for deformable objects via transformer," *arXiv preprint arXiv:2112.06374*, 2021.
- [23] A. S. Yenicesu, B. Cicek, and O. S. Oguz, "Fvit-grasp: Grasping objects with using fast vision transformers," *arXiv preprint arXiv:2311.13986*, 2023.
- [24] A. Gu and T. Dao, "Mamba: Linear-time sequence modeling with selective state spaces. arxiv 2023," *arXiv preprint arXiv:2312.00752*.
- [25] L. Zhu, B. Liao, Q. Zhang, X. Wang, W. Liu, and X. Wang, "Vision mamba: Efficient visual representation learning with bidirectional state space model," 2024. [Online]. Available: <https://arxiv.org/abs/2401.09417>
- [26] Y. Liu, Y. Tian, Y. Zhao, H. Yu, L. Xie, Y. Wang, Q. Ye, and Y. Liu, "Vmamba: Visual state space model," 2024. [Online]. Available: <https://arxiv.org/abs/2401.10166>
- [27] Z. Xing, T. Ye, Y. Yang, G. Liu, and L. Zhu, "Segmamba: Long-range sequential modeling mamba for 3d medical image segmentation," 2024. [Online]. Available: <https://arxiv.org/abs/2401.13560>
- [28] J. Ruan and S. Xiang, "Vm-unet: Vision mamba unet for medical image segmentation," 2024. [Online]. Available: <https://arxiv.org/abs/2402.02491>
- [29] H. Karaoguz and P. Jensfelt, "Object detection approach for robot grasp detection," in *2019 International Conference on Robotics and Automation (ICRA)*. IEEE, 2019, pp. 4953–4959.
- [30] D. Guo, F. Sun, H. Liu, T. Kong, B. Fang, and N. Xi, "A hybrid deep architecture for robotic grasp detection," in *2017 IEEE International Conference on Robotics and Automation (ICRA)*. IEEE, 2017, pp. 1609–1614.
- [31] Z. Zhou, S. Wang, Z. Chen, M. Cai, and Z. Kan, "A robotic visual grasping design: Rethinking convolution neural network with high-resolutions," *arXiv preprint arXiv:2209.07459*, 2022.
- [32] X. Qin, W. Hu, C. Xiao, C. He, S. Pei, and X. Zhang, "Attention-based efficient robot grasp detection network," *Frontiers of Information Technology & Electronic Engineering*, vol. 24, no. 10, pp. 1430–1444, 2023.
- [33] M. Zou, X. Li, Q. Yuan, T. Xiong, Y. Zhang, J. Han, and Z. Xiao, "Robotic grasp detection network based on improved deformable convolution and spatial feature center mechanism," *Biomimetics*, vol. 8, no. 5, p. 403, 2023.
- [34] Y. Gu, D. Wei, Y. Du, and J. Cao, "Cooperative grasp detection using convolutional neural network," *Journal of Intelligent & Robotic Systems*, vol. 110, no. 1, pp. 1–14, 2024.